

RSC Advances



This is an *Accepted Manuscript*, which has been through the Royal Society of Chemistry peer review process and has been accepted for publication.

Accepted Manuscripts are published online shortly after acceptance, before technical editing, formatting and proof reading. Using this free service, authors can make their results available to the community, in citable form, before we publish the edited article. This *Accepted Manuscript* will be replaced by the edited, formatted and paginated article as soon as this is available.

You can find more information about *Accepted Manuscripts* in the [Information for Authors](#).

Please note that technical editing may introduce minor changes to the text and/or graphics, which may alter content. The journal's standard [Terms & Conditions](#) and the [Ethical guidelines](#) still apply. In no event shall the Royal Society of Chemistry be held responsible for any errors or omissions in this *Accepted Manuscript* or any consequences arising from the use of any information it contains.

Cite this: DOI: 10.1039/c0xx00000x

www.rsc.org/xxxxxx

ARTICLE TYPE

Photoluminescence study of optically active Diaminopyridine intercalated Graphene oxide

Abhisek Gupta, Bikash Kumar Shaw and Shyamal Kumar Saha*

Received (in XXX, XXX) Xth XXXXXXXXXX 20XX, Accepted Xth XXXXXXXXXX 20XX

DOI: 10.1039/b000000x

Di-amino pyridine (DAP) ligand is successfully intercalated in GO layers to achieve layered type structure with interlayer separation ~ 1.03 nm. Density functional theory (DFT) is also carried out to investigate the stability of the modified structure along with its interlayer separation which agrees well with the experimental results. As synthesized di-amino pyridine functionalized GO (DAP-fGO) composites show better photoluminescent (PL) property compared to GO via surface passivation. Experimental observation of excitation dependent PL spectra of DAP-fGO composite is further verified by the DFT calculations of HOMO-LUMO band gaps. We believe that this study will help to design different GO-based nanomaterials with potential physical, chemical and optical applications.

Introduction

Graphene, being a zero band gap semiconductor, has attracted great research attention and technological interest in the fields of physics, chemistry and materials science¹⁻³ because of its unique electronic, thermal and mechanical properties⁴⁻⁶. However, due to absence of band gap, graphene cannot be used in digital logic performing devices where a band gap is required to provide distinct 'on' and 'off' state⁷. To overcome this limitation of the low on/off ratio, we have reported new types of graphene/graphene oxide (GO) based intercalated structures of different interlayer separations in our previous works⁸⁻¹⁰. Although graphene possesses versatile applications in several areas such as magnetic¹¹, electrical¹² and electrochemical applications¹³; it remains quite unexplored in the field of optical application due to its poor optical property generated from zero band gap characteristics. Oxygen rich graphene derivative such as graphene oxide (GO) possesses a finite electronic band gap generated due to the disruption of π networks. These oxygen enriched functional groups of GO (such as epoxy, hydroxyl, and carboxyl) can be considered as reactive sites for the tuning of its chemical and physical properties. GO, due to its layered type of structure and chemical reactive sites, undergoing intercalation by suitable molecules resulting one-dimensional expansion along its z-axis¹⁴. The concept of tailoring the interlayer distance between GO sheets is of great importance. Compared to its very high perspectives, very limited graphene-based hybrid materials with new structural and functional properties have recently been prepared through the intercalation of various molecules/ species such as amino acids, primary aliphatic amines, diaminoalkanes, polymers, ammonium ions, silica spheres and isocyanates in GO layers¹⁵⁻²¹. In our previous works⁹⁻¹⁰, to tune the GO interlayer separation,

we have intercalated GO by azo-pyridine and aminoazo-benzene ligands which mainly involves the reaction of the active carbon centers of the phenolic moieties present at the edges of GO. In the present study, we report on the successful intercalation of di-amino pyridine (DAP) ligand in GO layers without the aid of any coupling agent to develop novel 'N-crosslinked' nano-carbon hybrid material (DAP-fGO). Detailed FTIR and XPS spectroscopic measurements revealed the formation of covalent bonds between the intercalated DAP molecules and the GO sheets. DFT study is used to investigate the stability of the modified DAP-fGO composite structure along with its interlayer separation. As synthesized DAP-fGO composites show better photoluminescent (PL) property compared to GO via surface passivation. Experimental observation of excitation dependent PL spectra of DAP-fGO composite is further verified by the DFT calculations of HOMO-LUMO band gaps. This combined experimental and theoretical study of the electronic structure of DAP-fGO composite as a function of chemical modification of graphene provides a valuable information for the fabrication of tailored GO-based nanomaterials with improved chemical and physical properties.

Experimental sections

Chemicals

2,6-diaminopyridine (Merck), sodium chloride (Merck), ultrafine graphite powder (Loba), potassium permanganate (Merck), concentrated sulfuric acid (Merck, 98% pure), hydrogen peroxide (30%, Merck), hydrochloric acid (35%, Merck), methanol (99.9%, Merck) and double distilled water are used without further purification.

Synthesis

GO is synthesized from natural graphite by modified Hummers method²². In a typical experiment, X mg of DAP (X= 15, 30, 45) was dissolved in a 50 ml of ethanol and the freshly prepared solution was added drop wise to a 10 ml suspension of GO under vigorous stirring. The reaction was continued for 24 h at room temperature. During this reaction the mixture was protected from light. The as-synthesized DAP-fGO-X (X= 15, 30, 45) composite was isolated from the solution by centrifugation and washed thoroughly with 1:1 ethanol/water (30 ml, 4 times) to remove all unreacted compounds. The final product is dried overnight under vacuum at 80°C.

Characterization

To characterize the final product, powder X-ray diffraction (XRD) measurements are carried out using X-ray diffractometer (RICH SEIFERT-XRD 3000P with X-Ray Generator-Cu, 10 kV, 10 mA, wavelength 1.5418 Å). For the TEM study, we used a JEOL-2011 high resolution transmission electron microscope. Raman spectra are obtained from a micro-Raman spectrometer (Model: JYT-6400). The sample for Raman measurements was excited at 514 nm. FTIR spectroscopic measurements are carried out using a NICOLET MAGNA IR 750 system. The X-Ray Photoelectron Spectroscopy (XPS) is investigated using OMICRON-0571 system. DFT analysis regarding the total energies and molecular orbital (MO) calculation of the optimized composite structures are done with B3LYP/ 6-31G levels of theory using the standard program in the Gaussian 03 software package. UV-VIS absorption spectra are measured with a Cary UV 5000 spectrophotometer. PL spectra and photostability are investigated using Horiba Jobin Yvon Fluoromax-4 spectrofluorometer with a xenon lamp. The sample was excited continuously at excitation wavelength 340 nm for 1200 s to collect the fluorescence emission intensities every 120 s at the corresponding optimal emission wavelength.

Results and Discussion

X-Ray diffraction (XRD) study is a powerful and widely used tool for the characterization of layered materials. We have performed powder XRD study of our DAP-fGO samples to investigate the intercalation of DAP molecules in the graphene layers. DAP-fGO-45 composite shows diffraction peaks at 2θ value of 8.6°. For GO the peak appears at 2θ value of ~ 12.4° (interlayer separation ~ 0.719 nm). The shifting of peak to lower 2θ values compared to the corresponding peak of starting GO is unambiguously ascribed to an increase in interlayer separation [XRD study of GO, DAP-fGO-15 and 30 are shown in supporting Information]. According to the Bragg's law, the value of the interlayer separation is found to be 1.03 nm with an overall increase of the GO interlayer separation of about 0.309 nm compared to the starting GO. The full-width-at-half maximum (FWHM) value of the diffraction peak in the XRD pattern of the DAP-fGO-45 derivative was found to be much higher than the corresponding value of the pristine GO sample indicating the intercalation of DAP molecules in GO layers.

The Debye-Scherrer equation has been employed to estimate the mean crystallite thickness of the DAP-fGO-45 composite:

$$t = K\lambda / \text{FWHM} \cos\theta \dots (1)$$

where t is the mean crystallite thickness, K is a dimensionless shape factor with a value of about 0.9, λ is the wavelength of the X-ray used (λ= 1.5418 Å), θ is the angular position of the peak and FWHM is the full width at half maximum obtained from the graph (expressed in radians). The value of the average crystallite thickness for DAP-fGO-45 composite is ~37.5 Å. The number of layers (N) considering the lattice spacing as d is:

$$N = t/d \dots (2)$$

Taking t as 37.5 Å the number of layers for DAP-fGO-45 composite has been found to be ~4.

Figure 1b shows the TEM images of DAP-fGO-45 composite

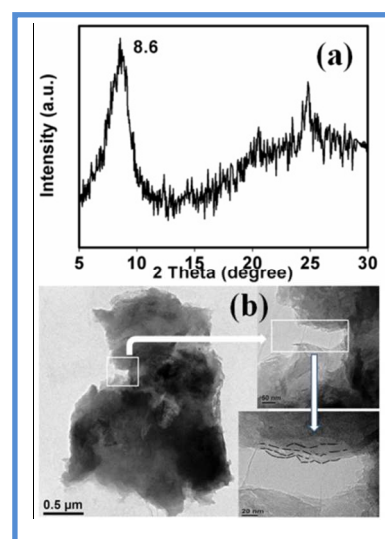


Fig. 1 (a) XRD pattern and (b) TEM images of DAP-fGO composite

taken at three different magnifications from which it is seen that 4-5 GO layers are stacked together to form a composite layered structure as estimated from the XRD analysis. This type of stacking of GO layers due to functionalization by potentially cross-linking agents has also been reported by other workers^{18, 23}. The functionalization of GO with DAP molecule is further confirmed by the FTIR analysis. Figure 2a shows the FTIR spectra for GO and DAP-fGO-45 composites. (FTIR profiles of DAP-fGO-15 and DAP-fGO-30 composites are shown in supporting information.) Pure dried GO exhibits the usual peaks at 3432, 1702, 1628, 1400, and 1067 cm⁻¹ corresponding to the hydrogen-bonded O-H stretching, carbonyl (C=O) stretching, C=C stretching, O-H deformation, and C-O stretching of the epoxides (C-O-C), respectively. In the DAP-fGO-45 composite, the peak at 3430 cm⁻¹ is due to the combined effect of the -OH and -NH groups. The combined effect of skeletal C=C vibration and pyridinic C=N vibrations is observed at 1624 cm⁻¹. It is also seen from the FTIR analysis that the epoxy group is disappeared in the composite while some new peaks at 1564, 1248 and 1047 cm⁻¹ corresponding to amine NH bending, C-N stretching and C-O stretching vibrations are appeared. These results confirm that DAP molecules react with the oxygen-containing functional

groups of GO, generating C–N covalent bonds through the nucleophilic addition reaction of amine and epoxy.

Raman spectroscopy, due to high sensitivity on electronic structures, is a powerful non-destructive tool to characterize ordered and disordered structures of carbon materials. Figure 2b shows the Raman spectra of GO and DAP-fGO-45 composite. The Raman spectra of GO

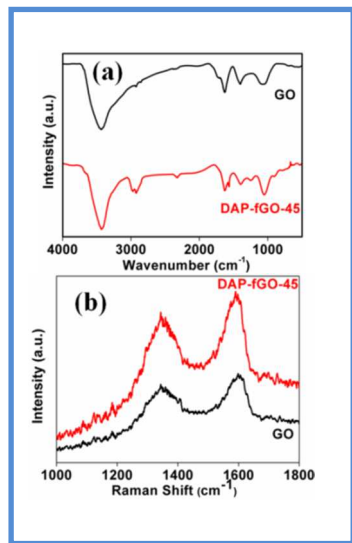


Fig. 2 (a) FTIR and (b) RAMAN spectra of GO and DAP-fGO composite

shows the characteristic G band at 1600 cm^{-1} , which corresponds to the first-order scattering of the E_{2g} phonon of in-plane vibration mode of sp^2 carbon atoms, and D band at 1345 cm^{-1} , which originates from the structural defects and partially disordered structures of the sp^2 domains and includes the vibration contributions of sp^3 -hybridised domains²⁴. However, for the DAP-fGO-45 composite, the G band is red-shifted to 1592 cm^{-1} while the D band is blue shifted to 1348 cm^{-1} . This type of shifting in binding energies of D and G bands has also been reported in some functionalized graphitic materials²⁵. The intensity ratio of D/G bands (I_D / I_G) is a measure of the disorder and reveals the degree of in-plane defects and edge defects in the carbon materials²⁶. In the present study, the I_D / I_G ratio of the DAP-fGO-45 composite is calculated to be ~ 0.909 , which is slightly smaller than that of the initial GO (~ 0.927). This observation implies the increase of the domain size of sp^2 carbon atoms in the DAP-fGO-45 composite due to the nucleophilic addition of the amino groups of DAP molecules to GO and the subsequent formation of covalent bonds.

We have analyzed the XPS spectra of GO and DAP-fGO-45 composite to find out the binding energies of the bonds present in GO and the composite. For GO (XPS spectra shown in Figure S4 of the Supporting Information), the low-range XPS spectra (Figure S4a) show the presence of only C and O 1s core-level photoemission peaks whereas the XPS spectrum of DAP-fGO-45 composite (Figure 3a) shows the characteristic C 1s, N 1s, and O 1s core-level photoemission peaks at ~ 285 , ~ 399 , and $\sim 532\text{ eV}$, respectively. From the XPS analysis, the C: O: N ratio has been found to be approximately $\sim 0.64:0.32:0.04$, which is close to the

C: N ratio ($\sim 0.62:0.05$) estimated from the elemental analysis. The high-resolution carbon 1s XPS spectrum of GO is conveniently fitted by three peaks at 284.8, 286.8, and 288.1 eV corresponding to C–C, C–O (hydroxyl and epoxides), and C=O (carboxyl) groups of GO¹⁰, whereas the high-resolution carbon 1s XPS spectrum of the DAP-fGO-45 composite shown in Figure 3b is deconvoluted into five components. The binding energy component at 284.87 eV is typically attributed to the C–C bond of the graphitic network^{27a} while the peaks at 285.79 and 286.3 eV originated from the C–N²³ and C=N^{27b} bonds respectively. Another component at 286.5 eV accounts for the C–O^{27a, c} bonds, and the highest binding energy peak at $\sim 288.8\text{ eV}$ is mainly assigned to the presence of carboxylic groups¹⁸.

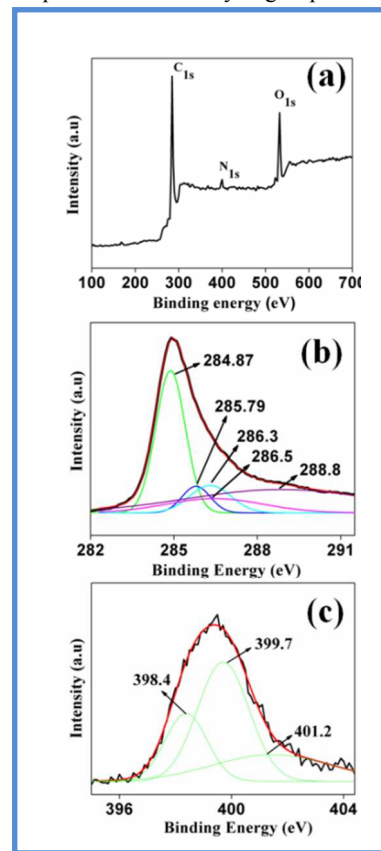


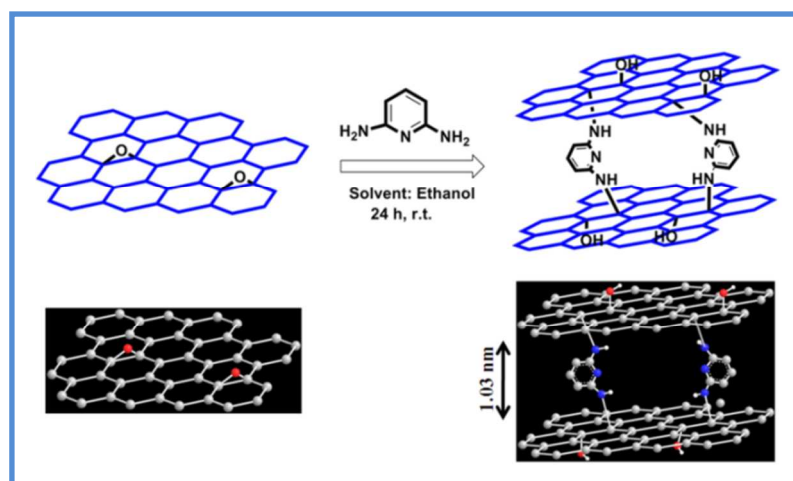
Fig. 3 (a) Low range XPS spectra (b) High resolution deconvoluted XPS peaks for C-1s and (c) for N-1s of DAP-fGO composite

To understand the chemical nature of nitrogen in DAP-fGO-45 composite is of great importance as it may provide useful information about the interactions between GO sheets and the nitrogen-containing groups of intercalated DAP. Figure 3c represents the high-resolution nitrogen 1s XPS spectrum which has been fitted by three components. The lower binding energy component at 398.4 eV ^{27d} is attributed to C=N bonds of pyridine and a second dominant peak, due to the presence of amine groups is observed at $\sim 399.7\text{ eV}$ ^{23, 27d}. The appearance of this component is assigned to the grafting of the amine-containing DAP into the GO framework. The higher binding energy component of the DAP-fGO-45 spectrum (401.2 eV) arises due to protonated amine groups^{27e}. Previous studies by other workers on intercalation of

Cite this: DOI: 10.1039/c0xx00000x

www.rsc.org/xxxxxx

ARTICLE TYPE



Scheme 1 Schematic diagram of the formation of DAP-fGO composite

amine-containing species in GO^{18,23} also show this type of protonated group which appears due to unavoidable exposure to air/electron beams during sample preparation and XPS measurements¹⁸.

Therefore, XRD, FTIR, Raman and XPS analysis suggest that the intercalation of DAP molecules into GO layers seems to occur entirely through a nucleophilic ring-opening reaction of the epoxy groups situated at the basal plane of GO (shown in Scheme 1). The ring-opening amination reaction of the epoxy group as a result of attack by nucleophiles (here the amino groups of DAP molecules) has been well documented for reactions between GO and amino-containing molecules as well as for intercalation reactions.

Figure 4a represents the combined UV-Vis absorption spectrum and PL spectra under variable excitation wavelengths for DAP-fGO-45 composite [Detailed Optical study of GO, DAP-fGO-15, 30 and 45 are given in supporting information]. From UV-Vis spectrum of the composite, a broad absorption region was observed with two peaks at ~235 and 335 nm. These two peaks are assigned to the π - π^* and n - π^* transitions of the composite. Moreover, in DAP-fGO-45 composite we observed an excitation wavelength dependent PL modulation. With the red shifting of excitation wavelength the emission peak intensity in the longer wavelength region (~490-500 nm) got intensified whereas the peak intensities in the blue region got suppressed. This trend in PL emission pattern and UV absorption in the composite can be attributed to amino functionalization of graphene oxide which improve the emission efficiency of the sp^2 domains of GO nanosheets^{28,29,30} by removing the non-radiative recombination inducing reactive sites such as the epoxy groups on the basal plane of GO via nucleophilic ring-opening amination reaction.

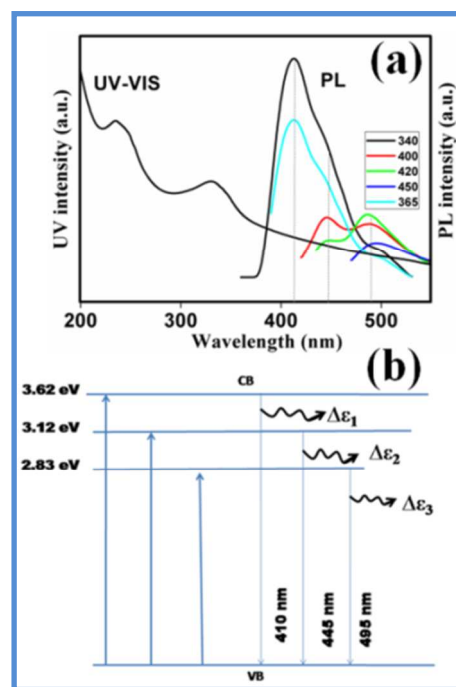


Fig. 4 (a) UV-VIS Spectra and Excitation dependent PL spectra of DAP-fGO composite, (b) Probable scheme for this PL mechanism

Due to the presence of discrete sp^2 C=C carbon domains and various functional groups such as amino, hydroxyl, carboxylic groups different electronic transition states will appear due to bonding and anti-bonding of molecular orbitals. This tunable PL can be attributed to the band to band (π^* - π transition) and interstate to band transitions (n - π transitions) resulting from

amino, hydroxyl, carboxylic group functionalization. Generally $\pi^*-\pi$ transitions dominated at lower wavelength region. As excitation wavelength gradually increased to higher region, $n-\pi$ transitions dominated and $\pi^*-\pi$ transitions got suppressed.

Here, a probable scheme for this PL mechanism has been proposed below. At a particular excitation wavelength it is assumed that ϵ is the energy corresponding to the radiative emission. It is also assumed that $\epsilon^+ > \epsilon > \epsilon^-$ where ϵ^+ and ϵ^- denotes the higher and lower radiative emission energies respectively. Now the total radiative emission energy of the system $E = f(\epsilon)$.

Therefore, the total radiative energy at lower wavelength region:

$$[\epsilon^+_{\pi^*-\pi} + \epsilon_{n-\pi} + \epsilon^-_{n-\pi}] = E \dots (1)$$

However, taking into consideration the possibility of the presence of some sort of non-radiative groups along with the amino, hydroxyl, carboxylic groups, and an extra term $-\Delta\epsilon$ ($\Delta\epsilon_1$, $\Delta\epsilon_2$, $\Delta\epsilon_3$) is incorporated in equation (1) due to this quenching probabilities of the non-radiative groups. $\Delta\epsilon$ represents total quenching component within the energy gap due to non-radiative species (assuming that the quenching bands lie within the energy band).

Therefore, $E = f(\epsilon, \Delta\epsilon)$.

Now equation (1) takes the following form at lower wavelength region:

$$[\epsilon^+_{\pi^*-\pi} + \epsilon_{n-\pi} + \epsilon^-_{n-\pi}] - \Delta\epsilon_1 = E \dots (2)$$

As excitation wavelength is shifting towards visible region, it can be modified as follows:

$$[\epsilon_{n-\pi} + \epsilon^-_{n-\pi}] - \Delta\epsilon_2 = E \dots (3)$$

Finally, at higher wavelength region the equation can be modified as:

$$\epsilon^-_{n-\pi} - \Delta\epsilon_3 = E \dots (4)$$

These equations clearly depict the excitation wavelength dependent heterogeneous PL modulation resulting from amino, hydroxyl, carboxylic group functionalization, which is in accordance with our proposed energy band diagram model as shown in figure 4b.

Detailed DFT Calculation:

For Theoretical study, we have started with bi-layer GO structure into which diamine pyridine molecules are sandwiched. Intercalated structures are optimized in steps with increasing number of DAP molecules to obtain the stable DAP-intercalated graphene structure. We have also shown how stabilization energies are altered upon addition of different functional groups into this stable parent optimized structure. The HOMO-LUMO energy levels and the generation of additional band gaps due to the addition of functional groups are calculated.

To begin with, we take an extended bi-layer 2-D graphene sheet, functionalized with one DAP molecule. The amine groups of the DAP molecule are attached to the active carbon centers of the

epoxy moieties of two graphene sheets via ring-opening amination reaction. After optimization to acquire stable DAP-intercalated graphene structure three molecules of DAP are required, as shown in Figure 5. The optimized structure shows the energy value of -5522.33 hartree unit. For this optimized structure, the two-dimensional graphene sheets are slightly displaced outward from the plane because of the bonding with amino groups of the bifunctional DAP ligand. The bond lengths and bond angles of the optimized doped structure are summarized in Table 1.

Table 1 Bond lengths and bond angles of the optimized DAP-fGO composite structure

Bond length (Å)	N ¹⁵⁶ -C ⁸⁹ , N ⁵ -C ¹⁵⁸	C ²² -C ⁹³	C ²⁰ -C ¹¹⁵	C ²⁴ -C ⁹⁰
	1.448	10.505	10.556	10.613
Bond angle (deg)	C ¹³⁷ -N ¹⁵⁶ -C ⁸⁹	C ¹⁴⁷ -N ¹⁶² -C ¹³		
	132.73	134.24		

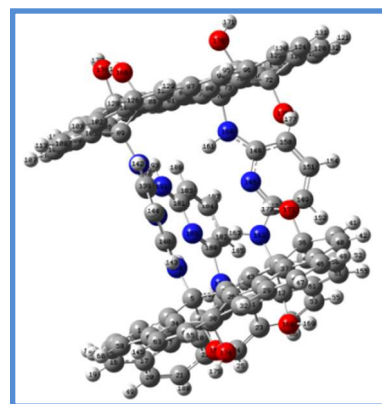


Fig. 5 Optimized structure of the DAP-fGO composite system

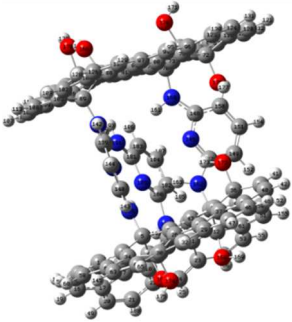
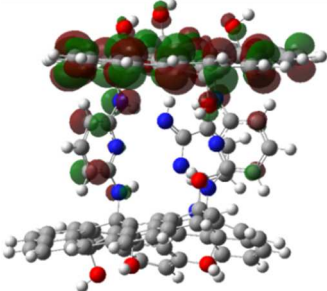
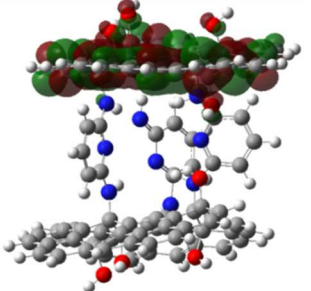
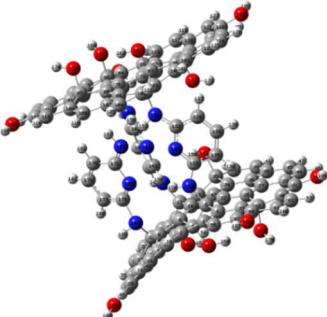
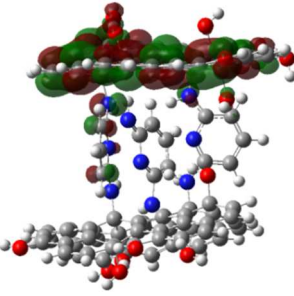
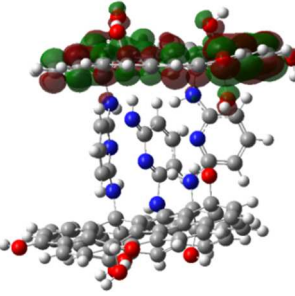
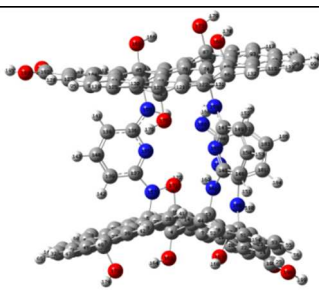
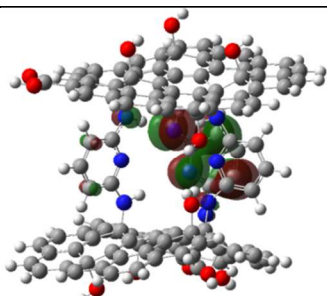
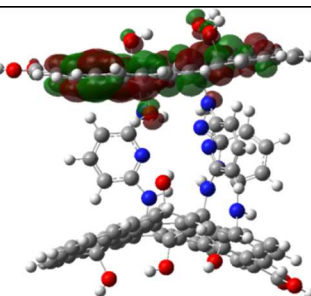
Its HOMO-LUMO molecular orbital pictures and energies are represented in Table 2. This DAP-intercalated graphene system shows the HOMO-LUMO band gap of around 3.62 eV. Using this structure as parent structure (1), we proceed to the next step of addition of functional groups (having non-bonded electron pairs) into it. The first shallow state is created by the addition of hydroxyl groups ($-\text{OH}$) to the surface of DAP-intercalated graphene. It is seen from the molecular orbital calculations that its (2) optimized structure generates the band gap of about 3.12 eV. Consequently, we see that the daughter system having more non-bonded electron rich groups shows smaller band gap. Considering this effect, we have incorporated carboxyl groups ($-\text{COOH}$) in place of hydroxyl groups in the parent structure to see whether same trend follow or not. In fact, carboxyl group, having more number of non-bonded electron pairs due to presence of two oxygen moieties forms a shallow state of band gap ~ 2.83 eV (3). So, theoretically it has been observed that with incorporation of electron rich substituents such as hydroxyl, carboxylic groups in the DAP-fGO-45 composite framework, two additional band gaps originate due to increase in non-bonding shallow state levels

Cite this: DOI: 10.1039/c0xx00000x

www.rsc.org/xxxxxx

ARTICLE TYPE

Table 2 DFT predicted structures of DAP-fGO composite and their Band gaps and spatial arrangements of HOMO-LUMO and their energies

Structure	Band Gap	HOMO	LUMO
 <p>Parent structure (1)</p>	3.62 eV	 <p>-8.52 eV</p>	 <p>-4.90 eV</p>
 <p>Hydroxyl group enriched (2)</p>	3.12 eV	 <p>-8.342 eV</p>	 <p>-5.224 eV</p>
 <p>carboxylic group enriched (3)</p>	2.83 eV	 <p>-7.896 eV</p>	 <p>-5.064 eV</p>

of -OH and -COOH groups respectively and it has also been observed from the experimental PL modulation with change in excitation wavelength and as well as in the PL of annealed DAP-fGO-45 composite (figure S6b) where the PL humps corresponding to the electron rich substituent got suppressed. Atomic coordinates of all optimized structures of 1, 2, and 3 are given in supporting information.

Conclusions

We have described a convenient approach for the preparation of intercalated layered type structure by functionalizing GO sheets with di-aminopyridine (DAP) moiety. In the composites, the GO sheets are attached through amino moieties to achieve a layered type structure with an interlayer separation of 1.03 nm. The formation of DAP-fGO composites are further supported by a

detailed series of structural characterizations, such as XRD, Raman spectroscopy, FTIR, XPS analysis. Structural stability and interlayer separation is confirmed using DFT calculation. This intercalated layered type functionalized GO composite shows better optical properties compared to GO via surface passivation. Excitation dependent PL spectra of DAP-fGO composite are further supported by the DFT calculations. The present investigation provides a combined way for the experimental and theoretical study of the electronic structure of DAP-fGO composite as a function of chemical modification of novel 'N-crosslinked' graphene oxide which gives valuable information to researchers to fabricate different GO-based nanomaterials with potential physical, chemical and optical applications.

Acknowledgements

AG and BKS acknowledge CSIR, New Delhi, for awarding fellowship and SKS acknowledges DST, project no. SR/S2/CMP-0097/2012.

Department of Materials Science, Indian Association for the Cultivation of Science, Jadavpur, Kolkata 700032, India, Email: cnssks@iacs.res.in

† Electronic Supplementary Information (ESI) available:

[Details of XRD, FTIR of DAP-fGO-15, 30; XRD, XPS and optical property (UV and PL and reason of optical property) of GO, and detailed optical measurements (PL, change of PL with pH and conc. change, photostability, atomic coordinates of all calculated structures) and are given in supporting information].

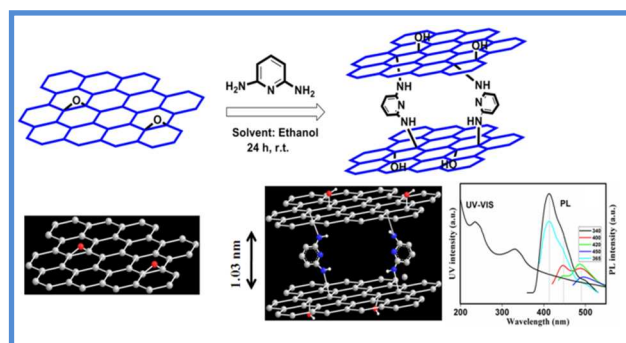
See DOI: 10.1039/b000000x

References

- 1 A. K. Geim, K. S. Novoselov, *Nat. Mater.*, 2007, **6**, 183
- 2 J. Wu, W. Pisula, K. Müllen, *Chem. Rev.*, 2007, **107**, 718
- 3 Y. Zhang, W. Y. Tan, L. H. Stormer, P. Kim, *Nature*, 2005, **438**, 201
- 4 A. Balandin, S. Ghosh, Z. W. Bao, I. Calizo, D. Teweldebrhan, F. Miao, N. C. Lau, *Nano Lett.*, 2008, **8**, 902
- 5 K. S. Novoselov, A. K. Geim, V. S. Morozov, D. Jiang, I. M. Katsnelson, V. I. Grigorieva, V. S. Dubonos, A. A. Firsov, *Nature*, 2005, **438**, 197
- 6 G. C. Lee, D. X. Wei, W. J. Kysar, J. Hone, *Science*, 2008, **321**, 385
- 7 P. Avouris, Z. Chen, V. Perebeinos, *Nat Nanotechnol.*, 2007, **2**, 605
- 8 M. Baskey and S. K. Saha, *Adv. Mater.*, 2012, **24**, 1589.
- 9 A. Gupta, S. K. Saha, *Nanoscale*, 2012, **4**, 6562–6567
- 10 A. Gupta, B. K. Shaw, S. K. Saha, *JPC C*, 2014, **118**, 6972
- 11 A. J. Akhtar, A. Gupta, D. Chakravorty and S. K. Saha, *AIP Advances*, 2013, **3**, 072124.
- 12 A. J. Akhtar, A. Gupta, B. K. Shaw, and S. K. Saha, *Appl. Phys. Lett.*, 2013, **103**, 242902
- 13 A. Gupta, A J Akhtar, S. K. Saha, *Mat Chem Phys.*, 2013, **140**, 616
- 14 M. Herrera-Alonso, A. A. Abdala, M. J. McAllister, I. A. Aksay, R. K. Prud'homme, *Langmuir*, 2007, **23**, 10644.
- 15 A. B. Bourlinos, D. Gournis, D. Petridis, T. Szabó, A. Szeri, and, I. Dékány, *Langmuir*, 2003, **19**, 6050
- 16 S. Stankovich, A. D. Dikin, C. O. Compton, B. H. G. Dommett, S. R. Ruoff, T. S. Nguyen, *Chem. Mater.*, 2010, **22**, 4153
- 17 W. S. Hung, C. H. Tsou, M. D. Guzman, Q. F. An, Y. L. Liu, Y. M. Zhang, C. C. Hu, K. R. Lee, and J. Y. Lai, *Chem. Mater.*, 2014, **26**, 2983
- 18 T. Tsoufis, F. Katsaros, Z. Sideratou, J. B. Kooi, M. A. Karakassides, and A. Siozios, *Chem. Eur. J.*, 2014, **20**, 8129
- 19 ZH Liu, ZM Wang, X Yang, K Ooi, *Langmuir*, 2002, **18**, 4926
- 20 Z. Lei, N. Christov, X. S. Zhao, *Energy Environ Sci.*, 2011, **4**, 1866
- 21 D. D. Zhang, Z. S. Zu, H. B. Han, *Carbon*, 2009, **47**, 2993

- 22 (a) D. Li, M. B. Mculler, S. Gilje, R. B. Kaner and G. G. Wallace, *Nat. Nanotechnol.*, 2008, **3**, 101; (b) N. I. Kovtyukhova, P. J. Ollivier, B. R. Martin, T. E. Mallouk, S. A. Chizhik, E. V. Buzaneva and A. D. Gorchinskiy, *Chem. Mater.*, 1999, **11**, 771
- 23 T. Tsoufis, G. Tuci, S. Caporali, D. Gournis, G. Giambastiani, *Carbon*, 2013, **59**, 100–108.
- 24 F. Tuinstra, L. J. Koenig, *J. Chem. Phys.*, 1970, **53**, 1126–1130
- 25 J. Yan, Y. Zhang, P. Kim, A. Pinczuk, *Phys. Rev. Lett.*, 2007, **98**, 166802.
- 26 Z. Jin, J. Yao, C. Kittrell, M. J. Tour, *ACS Nano*, 2011, **5**, 4112.
- 27(a) X-Z. Tang, W. Li, Z-Z Yu, M. A. Rafiee, J. Rafiee, F. Yavari, Nikhil Koratkar, *Carbon*, 2011, **49**, 1258; (b) U. Gelius, P. F. Heden, J. Hedman, B. J. Lindberg, R. Manne, R. Nordberg, C. Nordling, K. Siegbahn, *Phys. Scripta*, 1970, **2**, 70; (c) Y. Xue, Y. Liu, F. Lu, J. Qu, H. Chen, and L. Dai, *J. Phys. Chem. Lett.*, 2012, **3**, 1607; (d) B. J. Schultz, R. V. Dennis, J. P. Aldinger, C. Jaye, X. Wang, D. A. Fischer, A. N. Cartwright and S. Banerjee, *RSC Adv.*, 2014, **4**, 634; (e) I. V. Pavlidis, T. Vorhaben, T. Tsoufis, P. Rudolf, U. T. Bornscheuer, D. Gournis, H. Stamatis, *Bioresour. Technol.*, 2012, **115**, 164–171.
- 28 K. P. Loh, Q. Bao, G. Eda and M. Chhowalla, *Nat. Chem.*, 2010, **2**, 1015
- 29 G. Eda, Y. Lin, C. Mattevi, H. Yamaguchi, H. Chen, I. Chen, C. Chen and M. Chhowalla, *Adv. Mater.*, 2010, **22**, 505
- 30 Q. Mei, K. Zhang, G. Guan, B. Liu, S. Wang and Z. Zhang, *Chem. Commun.*, 2010, 46,7319

Table of Content



Optical property of daminopyridine intercalated GO composite with interlayer separation ~ 1.03 nm has been investigated by both experimental and theoretical approach.